Summary of speedups to be leveraged in MESA implementation of FRG24

Abstract

Here I summarize different ways to speed up the implementation of FRG24. Each section summarizes the steps that simplify the calculation, states how much it speeds things up by, and demonstrates the accuracy (or inaccuracy) of the new method. The first section is a TL;DR.

I. TL;DR AND THE STRUCTURE OF THIS DOCUMENT

Sec. II recaps the problem and lays out the starting point. In each subsequent section, I explain a way to speed up the calculation and how much of a speedup it provides.

The summary of each section and its speedup is as follows (note that calculating the eigenvalues of an $N \times N$ matrix goes like $O(N^3)$ complexity):

Sec. III. The matrix can be manipulated into a 2×2 block-diagonal structure, where each of the nonzero blocks is $N/2 \times N/2$ instead of $N \times N$. The complexity of calculating the eigenvalues of one block is therefore $\sim N^3/8$, so calculating all of the eigenvalues becomes $\sim N^3/4$, so **a factor of four speedup** without any approximations/errors whatsoever.

- One of these $N/2 \times N/2$ blocks is well-approximated by the HG19 model with slight-but-allowable (as I understand it) error. So if we just use HG19 for those eigenvalues, we only need to get the eigenvalues of one of these two blocks, so this gets **a factor of eight speedup**.

Sec. IV. For $\tau << 1$, one can show that the T equation is unnecessary and can be reduced to a simple relation between T and ψ that can be used to replace the T term in the momentum equation. This eliminates the T equation, thus removing a quarter of the rows/columns from the matrix, so the complexity of calculating the eigenvalues goes from $\sim N^3$ to $\sim (3/4)^3 N^3$ or **about a factor of two and one third speedup** while introducing errors of the order τ, which is tiny.

Sec. V. For small magnetic Reynolds number Rm, essentially identical manipulations allow the induction equation (the equation for A) to be eliminated and let us write the Lorentz force in terms of ψ. Combined with Sec. IV, this means half of the rows/columns have been removed from the matrix, so the complexity of calculating the eigenvalues goes from $\sim N^3$ to $\sim N^3/8$ or **a factor of eight speedup**. Unfortunately, while τ is always small in stars, it turns out that Rm is not always small, so this sometimes introduces non-trivial errors. However, I show that relying on HG19 allows us to keep these errors to within a factor of a few.

So, if we use all of these methods and are ok with some error, **the total speedup is a**

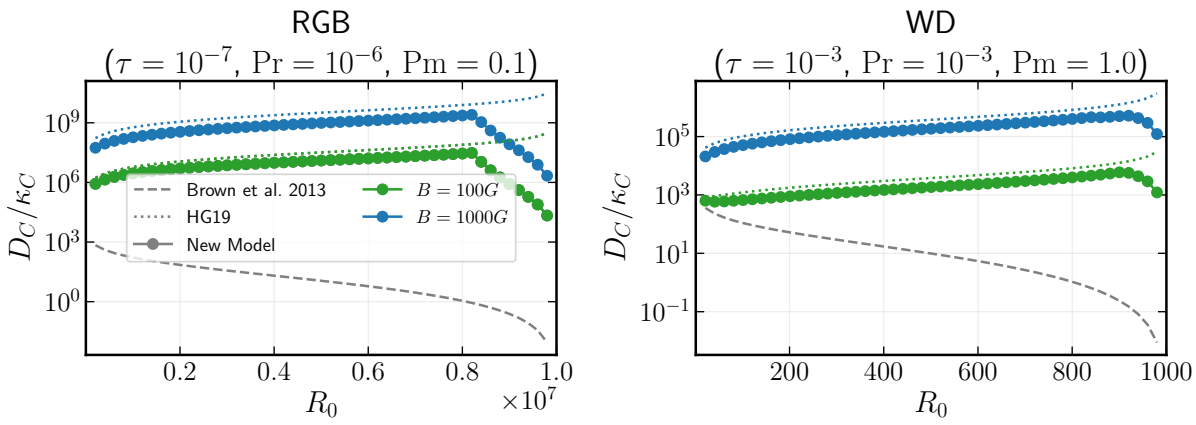

FIG. 1: (Figure copied from FRG24). Turbulent compositional diffusivity D_C normalized by microscopic diffusivity κ_C, predicted by various models, for parameter values appropriate of the fingering region of a typical RGB star (left) and a typical DA white dwarf (right), see FRG24 for detail. In each panel, the dashed grey line corresponds to the BGS13 hydrodynamic model, and the colored dotted lines correspond to the HG19 model. Finally, the round symbols correspond to the FRG24 model (labeled "New Model" here). The case for $B_0 = 100$G is shown in green and corresponds to $H_B = 10^{-7}$ for the RGB star, and $H_B = 10^{-3}$ for the white dwarf (cf. HG19). The case for $B_0 = 1000$G correspond to $H_B = 10^{-5}$ for the RGB star, and $H_B = 10^{-1}$ for the white dwarf.

factor of 64! If we want to play it safe and have only trivially small errors, we still get **almost a factor of 10 speedup**.

II. RECAP: OUR STARTING POINT, NO SIMPLIFICATIONS

The purpose of the FRG24 model is to calculate the chemical diffusivity of MHD fingering convection in a local radial shell provided fluid properties (Pr, τ, etc), gradients, and a magnetic field strength. We basically want to evaluate each point in Fig. 1 as quickly as possible in order for it to be useful to MESA users.

Evaluating the FRG24 model (i.e., any given point in Fig. 1) requires searching for the w_f that satisfies $\sigma(w_f) - C_2 * \lambda_f = 0$ (Eq. 28 in the final version of FRG24), where C_2 is a free parameter that we fit to DNS results. Finding this w_f requires evaluating σ for a number of values of w_f. Each evaluation of σ involves calculating the eigenvalues of a matrix

for a bunch of different wavenumbers k_z, and then taking the maximum real part of all the eigenvalues over all the k_z. The size of this matrix depends on the desired resolution (in x—details given in FRG24), so some speedups can be obtained by reducing resolution, and reducing the grid in k_z that we search over (here it would be helpful if we knew *a priori* what values of k_z we should limit our search to, which I think can be done using the matrix perturbation methods we use in QM, or as described in Algatheem et al GAFD 2023, DOI: 10.1080/03091929.2023.2268817). The following speedups I describe are independent of all that—I'm just focusing on tricks to make the calculation of the eigenvalues at a given w_f and k_z faster.

The linear system whose eigenvalues we need is given by Eqs. (41)-(44) of FRG24. They are repeated here for convenience, and note that I've done a tiny bit of algebra to simplify things:

$$\hat{\sigma}\hat{\psi}_m = i\frac{\hat{l}_f\hat{k}_z}{\hat{k}_m^2}\hat{E}_\psi\left[(\hat{l}_f^2-\hat{k}_{m+1}^2)\hat{\psi}_{m+1}+(\hat{l}_f^2-\hat{k}_{m-1}^2)\hat{\psi}_{m-1}\right] - \mathrm{Pr}\hat{k}_m^2\hat{\psi}_m - i\mathrm{Pr}\frac{m\hat{l}_f}{\hat{k}_m^2}(\hat{T}_m-\hat{C}_m)+iH_B\hat{k}_z\hat{A}_m, \quad (1)$$

$$\hat{\sigma}\hat{T}_m = -i\hat{l}_f\hat{k}_z\hat{E}_\psi(\hat{T}_{m+1}+\hat{T}_{m-1})-\hat{l}_f\hat{k}_z\hat{E}_T(\hat{\psi}_{m-1}-\hat{\psi}_{m+1})-im\hat{l}_f\hat{\psi}_m-\hat{k}_m^2\hat{T}_m, \quad (2)$$

$$\hat{\sigma}\hat{C}_m = -i\hat{l}_f\hat{k}_z\hat{E}_\psi(\hat{C}_{m+1}+\hat{C}_{m-1})-\hat{l}_f\hat{k}_z\hat{E}_C(\hat{\psi}_{m-1}-\hat{\psi}_{m+1})-im\hat{l}_f\frac{\hat{\psi}_m}{R_0}-\tau\hat{k}_m^2\hat{C}_m, \quad (3)$$

and

$$\hat{\sigma}\hat{A}_m = -i\hat{l}_f\hat{k}_z\hat{E}_\psi\left(\hat{A}_{m+1}+\hat{A}_{m-1}\right)-D_B\hat{k}_m^2\hat{A}_m+i\hat{k}_z\hat{\psi}_m. \quad (4)$$

Here $\hat{k}_m^2 \equiv m^2\hat{l}_f^2+\hat{k}_z^2$, and ψ_m, T_m, etc. result from a Fourier expansion in x of the form

$$\begin{pmatrix}\hat{\psi}_P\\ \hat{T}_P\\ \hat{C}_P\\ \hat{A}_P\end{pmatrix} = e^{\hat{\sigma}t+i\hat{k}_z z}\sum_{m=-N}^{N}\begin{pmatrix}\hat{\psi}_m\\ \hat{T}_m\\ \hat{C}_m\\ \hat{A}_m\end{pmatrix}e^{im\hat{l}_f x}, \quad (5)$$

so each m points to a different Fourier mode/component of the given field.

Pr, τ, R_0, H_B, and D_B are all model inputs that come from local gradients and fluid properties and such. l_f, E_ψ, E_T, and E_C are functions of those quantities (and of w_f) that we calculate separately and aren't important to repeat here—their precise definitions are given in FRG24. The above equations should be looked at as an eigenvalue problem of

the form $\mathbf{L}[\vec{f}] = \hat{\sigma}\vec{f}$ where $\vec{f}$ is all the different ψ_m, T_m, etc., and $\mathbf{L}$ is a big matrix whose coefficients depend on k_z, and we want to calculate its eigenvalues as efficiently as possible.

In what follows, it's helpful to recall that the complexity for calculating all the eigenvalues of an $N \times N$ matrix (assuming no linear algebra tricks, i.e., just using LAPACK out of the box) is $O(N^3)$.

III. FIRST SPEEDUP: CHANGE OF BASIS, BLOCK-DIAGONAL FORM

Noticing that the equations are littered with expressions of the form $f_{m+1} \pm f_{m-1}$, we can see what happens if, instead of writing our equations down in terms of ψ_m (and T_m, C_m, A_m), we write them down in terms of the quantities $\psi_m + \psi_{-m}$ and $\psi_m - \psi_{-m}$ (and likewise for T, C, and A) where $m = 1, 2, \ldots$ and we don't change the $m = 0$ case at all. This is just like switching from the $\{|\uparrow\rangle, |\downarrow\rangle\}$ basis to the $\{|\uparrow\rangle + |\downarrow\rangle, |\uparrow\rangle - |\downarrow\rangle\}$ one in QM, or you can view it as doing a sine/cosine transform in x rather than a Fourier transform.

For $m > 0$, define $\psi_{m\pm} \equiv \psi_m \pm \psi_{-m}$ (and likewise for T, C, and A). Then the equations can be rewritten as follows.

First, the $m = 0$ equations:

$$\hat{\sigma}\hat{\psi}_0 = i\frac{\hat{l}_f}{\hat{k}_z}\hat{E}_\psi(\hat{l}_f^2 - k_1^2)\hat{\psi}_{1+} - \mathrm{Pr}\hat{k}_z^2\hat{\psi}_0 + iH_B\hat{k}_z\hat{A}_0, \tag{6}$$

$$\hat{\sigma}\hat{T}_0 = -i\hat{l}_f\hat{k}_z\hat{E}_\psi\hat{T}_{1+} + \hat{l}_f\hat{k}_z\hat{E}_T\hat{\psi}_{1-} - \hat{k}_z^2\hat{T}_0, \tag{7}$$

$$\hat{\sigma}\hat{C}_0 = -i\hat{l}_f\hat{k}_z\hat{E}_\psi\hat{C}_{1+} + \hat{l}_f\hat{k}_z\hat{E}_C\hat{\psi}_{1-} - \tau\hat{k}_z^2\hat{C}_0, \tag{8}$$

$$\hat{\sigma}\hat{A}_0 = -i\hat{l}_f\hat{k}_z\hat{E}_\psi\hat{A}_{1+} - D_B\hat{k}_z^2\hat{A}_0 + i\hat{k}_z\hat{\psi}_0. \tag{9}$$

The $m = 1$ plus/minus the $m = -1$ equations are:

$$\hat{\sigma}\hat{\psi}_{1\pm} = i\frac{\hat{l}_f\hat{k}_z}{\hat{k}_1^2}\hat{E}_\psi\left[(\hat{l}_f^2 - k_2^2)\hat{\psi}_{2\pm} + (1 \pm 1)(\hat{l}_f^2 - k_z^2)\hat{\psi}_0\right] - \mathrm{Pr}\hat{k}_1^2\hat{\psi}_{1\pm} - i\mathrm{Pr}\frac{\hat{l}_f}{\hat{k}_1^2}(\hat{T}_{1\mp} - \hat{C}_{1\mp}) + iH_B\hat{k}_z\hat{A}_{1\pm}, \tag{10}$$

$$\hat{\sigma}\hat{T}_{1\pm} = -i\hat{l}_f\hat{k}_z\hat{E}_\psi\left[\hat{T}_{2\pm} + (1 \pm 1)\hat{T}_0\right] - \hat{l}_f\hat{k}_z\hat{E}_T\left[(1 \mp 1)\hat{\psi}_0 - \hat{\psi}_{2\mp}\right] - i\hat{l}_f\hat{\psi}_{1\mp} - \hat{k}_1^2\hat{T}_{1\pm}, \tag{11}$$

$$\hat{\sigma}\hat{C}_{1\pm} = -i\hat{l}_f\hat{k}_z\hat{E}_\psi\left[\hat{C}_{2\pm} + (1 \pm 1)\hat{C}_0\right] - \hat{l}_f\hat{k}_z\hat{E}_C\left[(1 \mp 1)\hat{\psi}_0 - \hat{\psi}_{2\mp}\right] - i\hat{l}_f\frac{\hat{\psi}_{1\mp}}{R_0} - \tau\hat{k}_1^2\hat{C}_{1\pm}. \tag{12}$$

$$\hat{\sigma}\hat{A}_{1\pm} = -i\hat{l}_f\hat{k}_z\hat{E}_\psi\left[\hat{A}_{2\pm} + (1\pm 1)\hat{A}_0\right] - D_B\hat{k}_1^2\hat{A}_{1\pm} + i\hat{k}_z\hat{\psi}_{1\pm}. \tag{13}$$

The equations for arbitrary m become:

$$\hat{\sigma}\hat{\psi}_{m\pm} = i\frac{\hat{l}_f\hat{k}_z}{\hat{k}_m^2}\hat{E}_\psi\left[(\hat{l}_f^2 - k_{m+1}^2)\hat{\psi}_{(m+1)\pm} + (\hat{l}_f^2 - k_{m-1}^2)\hat{\psi}_{(m-1)\pm}\right]$$
$$- \mathrm{Pr}\hat{k}_m^2\hat{\psi}_{m\pm} - i\mathrm{Pr}\frac{m\hat{l}_f}{\hat{k}_m^2}(\hat{T}_{m\mp} - \hat{C}_{m\mp}) + iH_B\hat{k}_z\hat{A}_{m\pm}, \tag{14}$$

$$\hat{\sigma}\hat{T}_{m\pm} = -i\hat{l}_f\hat{k}_z\hat{E}_\psi(\hat{T}_{(m+1)\pm} + \hat{T}_{(m-1)\pm}) + \hat{l}_f\hat{k}_z\hat{E}_T(\hat{\psi}_{(m+1)\mp} - \hat{\psi}_{(m-1)\mp}) - im\hat{l}_f\hat{\psi}_{m\mp} - \hat{k}_m^2\hat{T}_{m\pm}, \tag{15}$$

$$\hat{\sigma}\hat{C}_{m\pm} = -i\hat{l}_f\hat{k}_z\hat{E}_\psi(\hat{C}_{(m+1)\pm} + \hat{C}_{(m-1)\pm})$$
$$+ \hat{l}_f\hat{k}_z\hat{E}_C(\hat{\psi}_{(m+1)\mp} - \hat{\psi}_{(m-1)\mp}) - im\hat{l}_f\frac{\hat{\psi}_{m\mp}}{R_0} - \tau\hat{k}_m^2\hat{C}_{m\pm}, \tag{16}$$

$$\hat{\sigma}\hat{A}_{m\pm} = -i\hat{l}_f\hat{k}_z\hat{E}_\psi\left(\hat{A}_{(m+1)\pm} + \hat{A}_{(m-1)\pm}\right) - D_B\hat{k}_m^2\hat{A}_{m\pm} + i\hat{k}_z\hat{\psi}_{m\pm}. \tag{17}$$

If you stare at these equations for long enough, you see that they decouple into two separate subsystems: ψ_0 couples to A_0 and ψ_{1+} (but not T_0, C_0, or ψ_{1-}), and through them it couples to A_{1+} (but not A_{1-}), T_{1-} (but not T_{1+}), C_{1-} (but not C_{1+}), and ψ_{2+} (but not ψ_{2-}), and so on. So all eigenmodes of this system either have zero contribution from ψ_0, A_0, ψ_{m+}, A_{m+}, T_{m-}, C_{m-} and possibly nonzero contributions from T_0, C_0, ψ_{m-}, T_{m+}, C_{m+}, A_{m-}, or zero contribution from the latter and possibly nonzero contribution from the former. So, this is a 2×2 block-diagonal system.

If you can write a matrix as a block-diagonal of the form

$$\mathbf{L} = \begin{bmatrix} \mathbf{L}_1 & \mathbf{0} \\ \mathbf{0} & \mathbf{L}_2 \end{bmatrix}, \tag{18}$$

then the eigenvalues of $\mathbf{L}$ are simply the eigenvalues of the submatrices $\mathbf{L}_1$ and $\mathbf{L}_2$. If $\mathbf{L}$ is $N \times N$ and $\mathbf{L}_1$ and $\mathbf{L}_2$ are both $N/2 \times N/2$ (as is the case here), then calculating the eigenvalues of $\mathbf{L}$ would normally be $O(N^3)$ complexity, but if you instead calculate the eigenvalues of the individual blocks, then each block is $O((N/2)^3)$ complexity, so to get the eigenvalues of both blocks scales like $N^3/4$ ($N^3/8$ for one block plus $N^3/8$ for the other).

The fact that this method produces identical eigenvalues to the original system can be seen for one particular case in Fig. 2.

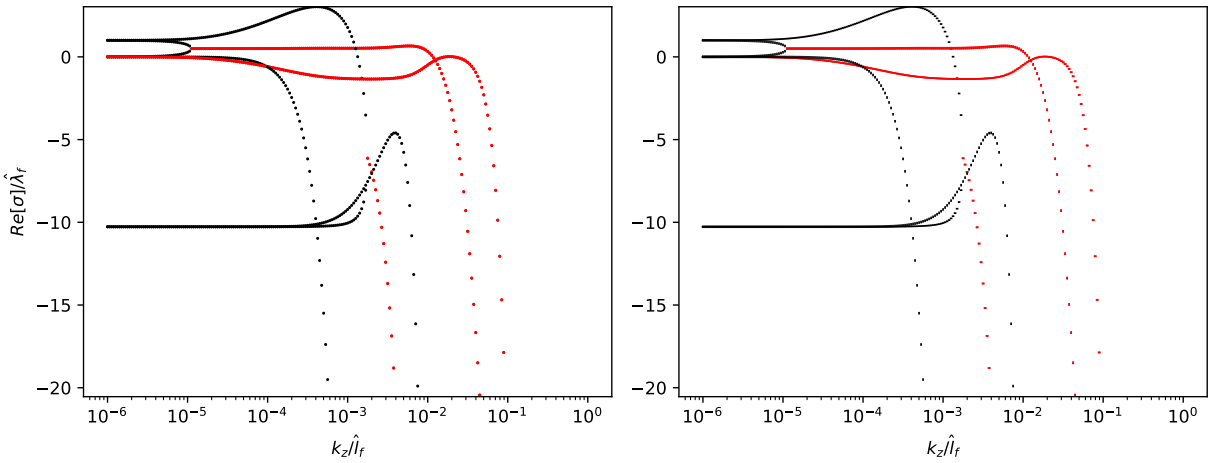

FIG. 2: For the physical parameters corresponding to the $100G$ RGB case in Fig. 1, and the w_f corresponding to $R_0 = 8 \times 10^6$, the real part of the eigenvalues $Re[\lambda]$ (normalized to the elevator mode growth rate λ_f) is plotted against wavenumber k_z for the full system Eqs. (1)-(4) (left) and for the two separate subsystems from the block-diagonal form (right). Black points are "direct" modes, i.e., $Im[\sigma] = 0$, and red points correspond to two complex-conjugate pairs of eigenvalues. On the right, eigenvalues corresponding to the $\psi_0, A_0 \neq 0$ block are given by vertical bars (might have to zoom in on the PDF to see the symbols clearly, sorry), and eigenvalues corresponding to the $T_0, C_0 \neq 0$ block by horizontal bars. The punchline is that they are identical, but the right panel is 4 times faster to calculate. Note that the global maximum (around $k_z/l_f \approx 4 \times 10^{-4}$) corresponds to one block while the local maximum that occurs near $k_z/l_f \approx 3 \times 10^{-3}$ and $\sigma/\lambda_f \approx -5$ (this branch will turn out to be important later) corresponds to the other block.

A. Using HG19 to approximate one of the blocks

Figure 2 demonstrates that there are multiple eigenvalue branches in this system, and that they can peak at different wavenumbers and with different peak growth rates. In the testing I've done so far (read: who knows whether or not there are edge cases that violate this general rule) I've found that, when the FRG24 and HG19 models are in reasonable agreement (so, for R_0 not too large, see Fig. 1), the branch that has the largest global maximum is the same one that's the largest in Fig. 2. Plotting the flows corresponding to this eigenmode reveals that they're very similar to the flows you typically get in KH with a sinusoidal shear flow, so let's refer to that branch as the **ordinary KH branch**.

On the other hand, whenever the FRG24 and HG19 models disagree significantly (large R_0), the branch that has the largest global maximum is the one that, in Fig. 2, peaks at around $k_z/l_f \approx 3 \times 10^{-3}$ and $\sigma/\lambda_f \approx -5$ (for these parameters, it has a negative growth rate and so it is decaying; but for larger R_0 this mode pops up and is more unstable than the ordinary KH branch). Plotting the flows corresponding to this mode shows they look like a weird kind of KH I've seen before, so let's call this branch the **weird KH branch**. Note that the ordinary and weird KH branches correspond to different blocks (in the right panel of Fig. 2, one is shown with vertical lines while the other is horizontal)!

Since the ordinary KH branch is well-approximated by the HG19 model, we arguably don't need to calculate those eigenvalues as long as we're ok with the degree of error in Fig. 1 at small/medium R_0. Then the speedup is a factor of 8, instead of a factor of 4.

IV. SECOND SPEEDUP: LOW-τ LIMIT

Xie et al Fluids 2017 [1] shows that, for $\tau \ll 1$, the dominant balance in the temperature equation is between diffusion and the term corresponding to advection of the background gradient by flow fluctuations—the last two terms in Eq. (2) above (this is sometimes called the low Péclet number limit and dates at least back to a 1958 paper by Malkus and Veronis, and is discussed in Pascale's 2021 review in Phys Rev Fluids). Equating these terms yields

$$\hat{T}_m = \frac{-im\hat{l}_f}{\hat{k}_m^2}\hat{\psi}_m, \tag{19}$$

which can be inserted into Eq. (1) to yield:

$$\hat{\sigma}\hat{\psi}_m = i\frac{\hat{l}_f\hat{k}_z}{\hat{k}_m^2}\hat{E}_\psi\left[(\hat{l}_f^2 - \hat{k}_{m+1}^2)\hat{\psi}_{m+1} + (\hat{l}_f^2 - \hat{k}_{m-1}^2)\hat{\psi}_{m-1}\right] - \mathrm{Pr}\left(\hat{k}_m^2 + \frac{m^2\hat{l}_f^2}{\hat{k}_m^4}\right)\hat{\psi}_m + i\mathrm{Pr}\frac{m\hat{l}_f}{\hat{k}_m^2}\hat{C}_m + iH_B\hat{k}_z\hat{A}_m, \tag{20}$$

$$\hat{\sigma}\hat{C}_m = -i\hat{l}_f\hat{k}_z\hat{E}_\psi(\hat{C}_{m+1} + \hat{C}_{m-1}) - \hat{l}_f\hat{k}_z\hat{E}_C(\hat{\psi}_{m-1} - \hat{\psi}_{m+1}) - im\hat{l}_f\frac{\hat{\psi}_m}{R_0} - \tau\hat{k}_m^2\hat{C}_m, \tag{21}$$

$$\hat{\sigma}\hat{A}_m = -i\hat{l}_f\hat{k}_z\hat{E}_\psi\left(\hat{A}_{m+1} + \hat{A}_{m-1}\right) - D_B\hat{k}_m^2\hat{A}_m + i\hat{k}_z\hat{\psi}_m. \tag{22}$$

(I have the block-diagonal version of this written in a separate overleaf to save space here, but am happy to insert it here if asked).

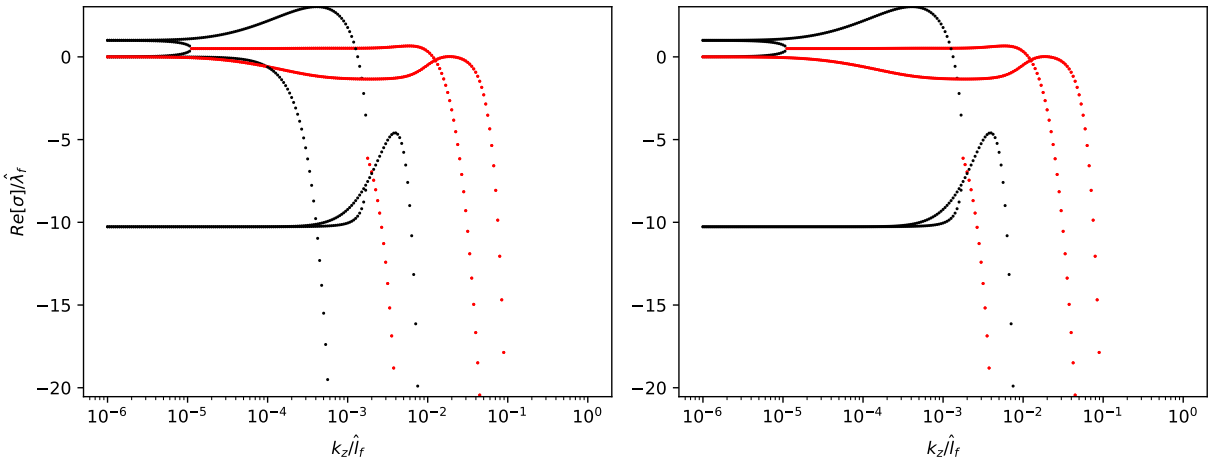

FIG. 3: Same as Fig. 2, but now the right panel shows the eigenvalues of Eqs. (20)-(22). Punchline: all the branches we care about are captured well, and the calculation is about 2.4 times faster.

The resulting system is smaller by a factor of 3/4 and should yield errors of order τ, which is tiny [2]. Figure 3 shows that the eigenvalues (for the branches we care about) are captured well by this approximation.

Since the eigenvalue complexity goes like N^3 and this reduces the size of the matrix by 3/4, this offers a speedup of a factor of $(4/3)^3 \approx 2.4$. This can be combined with the block-diagonalization of the previous section for a combined speedup of $(4/3)^3 \times 4 \approx 9.5$ if we calculate both blocks, or $(4/3)^3 \times 8 \approx 19$ if we rely on HG19 for the ordinary KH branch.

V. THIRD SPEEDUP: LOW-Rm LIMIT

Just as diffusion and advection of the background dominate in the T equation if τ is small, diffusion and advection of the background dominate in the A equation if the magnetic Reynolds number Rm is small (in talks I've seen this called "the quasi-static approximation", but I don't have a reference handy). Equating these last two terms in the A equation yields

$$\hat{A}_m = i\frac{\hat{k}_z}{D_B \hat{k}_m^2}\hat{\psi}_m, \tag{23}$$

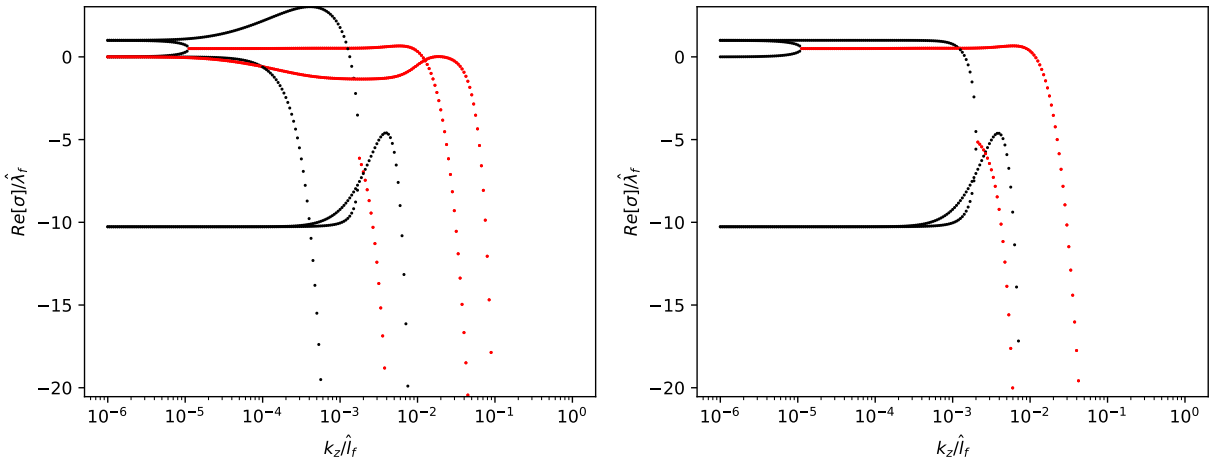

FIG. 4: Same as Fig. 3, but now the right panel shows the eigenvalues of Eqs. (24) and (25). Punchline: the weird KH branch is captured well, but not the ordinary KH branch. Combined with the small-τ limit, this matrix has half as many rows/columns and therefore calculating the eigenvalues is 8 times faster.

which can be inserted into the momentum equation to yield

$$\hat{\sigma}\hat{\psi}_m = i\frac{\hat{l}_f\hat{k}_z}{\hat{k}_m^2}\hat{E}_\psi\left[(\hat{l}_f^2-\hat{k}_{m+1}^2)\hat{\psi}_{m+1}+(\hat{l}_f^2-\hat{k}_{m-1}^2)\hat{\psi}_{m-1}\right] - \mathrm{Pr}\left(\hat{k}_m^2+\frac{m^2\hat{l}_f^2}{\hat{k}_m^4}+\frac{H_B\hat{k}_z^2}{D_B\hat{k}_m^2}\right)\hat{\psi}_m + i\mathrm{Pr}\frac{m\hat{l}_f}{\hat{k}_m^2}\hat{C}_m, \quad (24)$$

$$\hat{\sigma}\hat{C}_m = -i\hat{l}_f\hat{k}_z\hat{E}_\psi(\hat{C}_{m+1}+\hat{C}_{m-1}) - \hat{l}_f\hat{k}_z\hat{E}_C(\hat{\psi}_{m-1}-\hat{\psi}_{m+1}) - im\hat{l}_f\frac{\hat{\psi}_m}{R_0} - \tau\hat{k}_m^2\hat{C}_m, \quad (25)$$

(I have the block-diagonal version of this written in a separate overleaf to save space here, but am happy to insert it here if asked).

Unfortunately, Rm isn't an input parameter to our model and it's not clear which of multiple possible definitions of Rm needs to be small for this to be a valid approximation. Instead of dwelling on this, I've just gone and tested this approximation against the full model to see how it does. Figure 4 shows that this model does a great job of capturing the weird KH branch but not the ordinary KH branch, but the latter is reasonably captured by the HG19 model. Figure 5 corresponds to the WD case and shows that the weird KH branch isn't always captured beautifully by this model—but it's still there. Some back-of-the-envelope junk that I'm happy to expand upon leads me to suspect that the small-Rm limit does better the smaller $\mathrm{Pm}\tau/\mathrm{Pr}$ is.

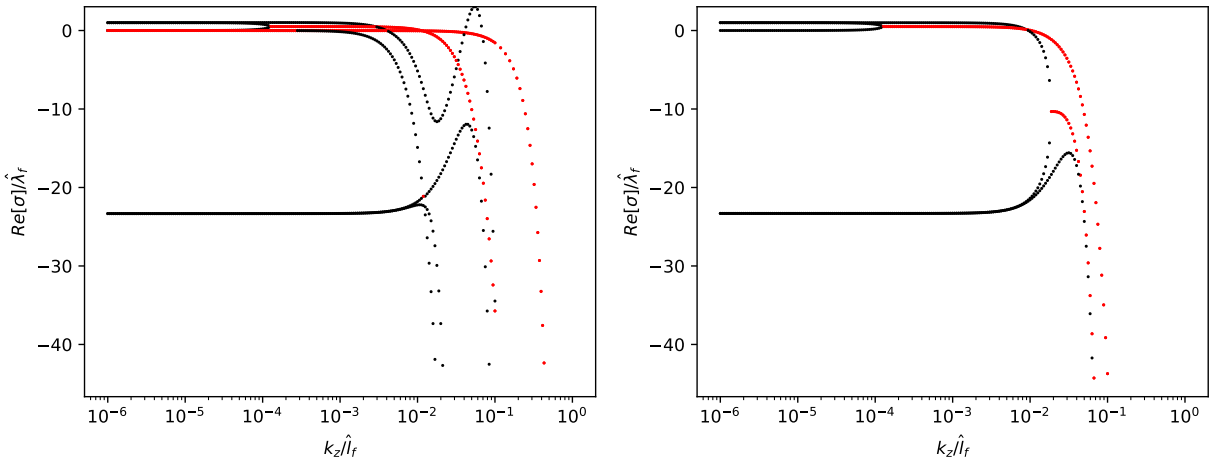

FIG. 5: Same as Fig. 4, but the parameters correspond to the $100G$ WD case depicted in Fig. 1, with $R_0 = 990$. Note that the weird KH branch is still captured, but not as well.

Since the low τ and low Rm limits combined remove the T and A equations, the system is now half the size, and calculating eigenvalues goes from N^3 to $(N/2)^3$, so the eigenvalues of this matrix are 8 times easier to calculate.

A. Getting around the issue of missing the ordinary KH branch

Figure 4 demonstrates that the system with T and A removed is able to capture the weird KH branch but not the ordinary KH branch. Recall that the weird KH branch is the one that matters at large R_0 where FRG24 and HG19 disagree in Fig. 1, while the ordinary KH branch is the one that matters whenever FRG24 and HG19 agree. So we have an issue: while Eqs. (24)-(25) are 8 times easier to solve than the original system (with another factor of 4 speedup provided by the block-diagonal stuff, or a factor of 8 if we only calculate one of the blocks), it seems they can only reliably get us the weird KH mode that dominates at large R_0. However, the ordinary KH mode is reasonably well-approximated by HG19.

I propose that, for every grid cell/timestep where we need to calculate a thermohaline diffusivity in MESA, we first calculate it using the HG19 model and then using the most reduced model I've presented here (which is 64 times faster if you use the block-diagonal stuff to calculate just one of the blocks, and then use the low-τ and low-Rm limits to cut the number of equations in half). If the HG19 model returns a smaller diffusivity, it means the

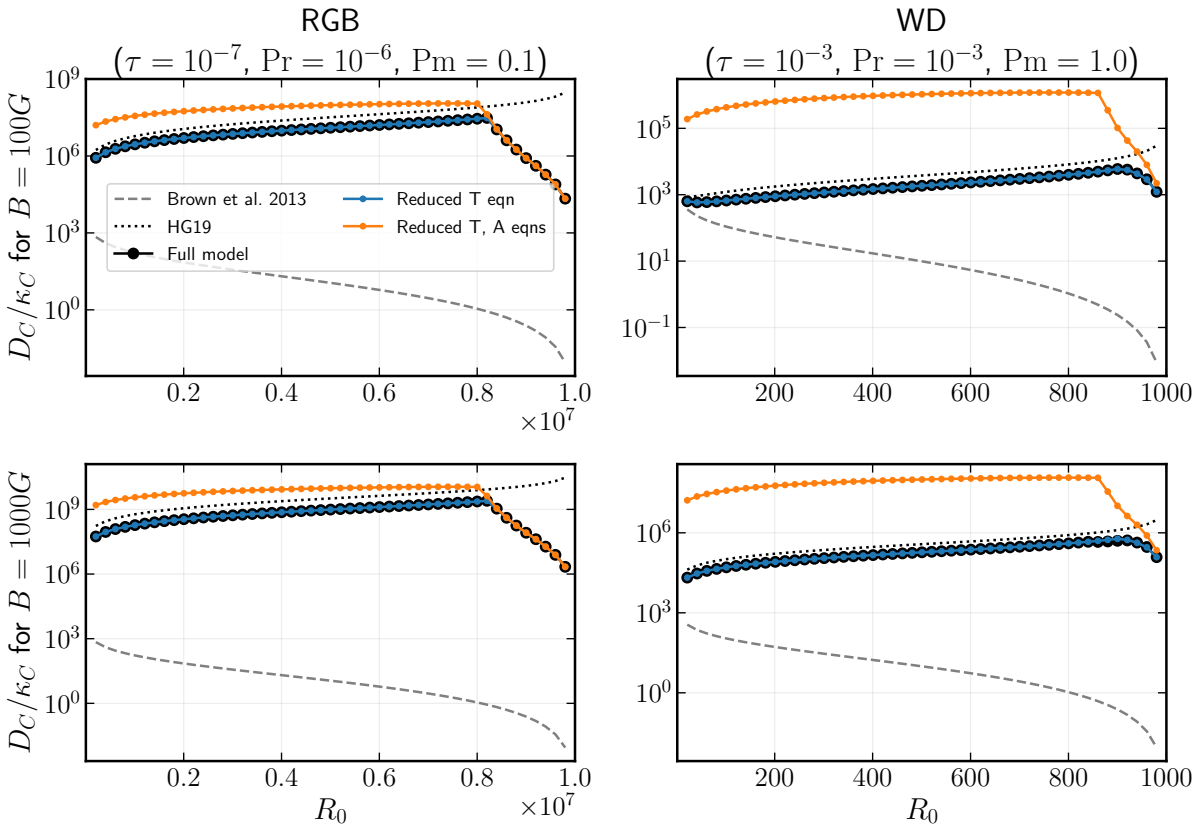

FIG. 6: Same as Fig. 1, but the top and bottom rows now correspond to the different magnetic field strengths, and different reductions of the fuller FRG24 model are compared. Grey dashed lines are the BGS13 hydro model, black thin dotted lines are HG19, large black circles are the full FRG24, blue circles are the low-τ limit, and orange circles are the low-τ and low-Rm limits combined. Note that, across the board, taking the minimum of the orange curve and the HG19 curve is a reasonable approximation to the full model. If someone wants to stay on the safe side, they can still use the blue curve (plus the block diagonalization stuff) to make the calculation much faster than the full model.

ordinary KH branch is dominant, and that we're in the regime where HG19 is a reasonable model. If the other diffusivity is smaller, it means the weird KH branch is dominant, and that we're in the regime where we should be using it instead of the HG19 result. You can see in Fig. 6 what would happen if you used this method to calculate the diffusivities considered in Fig. 1 by comparing the large black circles to the minimum between the HG19 curve and

the orange curve.

---

[1] Note they use a different nondimensionalization, so they have factors of τ and R_0 in different parts of their equations than we do.

[2] While nonnormal operators, which this certainly is, have the annoying feature that $O(\epsilon)$ perturbations to the coefficients sometimes drive $O(1)$ perturbations in the eigenvalues, that fortunately doesn't seem to be the case here